

Possible phonon-induced electronic bi-stability in VO₂ for ultrafast memory at room temperature

Cédric Weber,¹ Swagata Acharya,¹
Brian Cunningham², Myrta Grüning^{2,3}, Liangliang Zhang⁴
Hang Zhao⁵, Yong Tan⁵, Yan Zhang⁴, Cunlin Zhang⁴, Kai Liu⁶,
Mark Van Schilfgaarde,¹ Mostafa Shalaby⁴

¹King's College London, The Strand, WC2R 2LS London, UK,

²School of Mathematics and Physics, Queen's University Belfast, Belfast BT7 1NN, UK,

³European Theoretical Spectroscopy Facility (ETSF),

⁴Key Laboratory of Terahertz Optoelectronics, Beijing Advanced
Innovation Center for Imaging Technology CNU, Beijing 100048, China

⁵Beijing Key Laboratory for Precision Optoelectronic Measurement Instrument
and Technology, School of Optics and Photonics,
Beijing Institute of Technology, Beijing 100081, China

⁶School of Materials Science and Engineering,
Tsinghua University, Beijing 100084, China,

VO₂ is a model material system which exhibits a metal to insulator transition at 67°C. This holds potential for future ultrafast switching in memory devices, but typically requires a purely electronic process to avoid the slow lattice response. The role of lattice vibrations is thus important, but it is not well understood and it has been a long-standing source of controversy. We use a combination of ultrafast spectroscopy and ab initio quantum calculations to unveil the mechanism responsible for the transition. We identify an atypical

Peierls vibrational mode which acts as a trigger for the transition. This rules out the long standing paradigm of a purely electronic Mott transition in VO₂; however, we found a new electron-phonon pathway for a purely reversible electronic transition in a true bi-stable fashion under specific conditions. This transition is very atypical, as it involves purely charge-like excitations and requires only small nuclear displacement. Our findings will prompt the design of future ultrafast electro-resistive non-volatile memory devices.

Introduction

Optical bi-stability is a key property to achieve ultrafast logic memory and switching devices (1,2). It is typically obtained when two distinct but nearly degenerate electronic states coexist, and is controlled by some combination of electronic charge and spin, and their coupling to quantized lattice vibrations (phonons). Its application to binary data storage is determined by the transition and relaxation times between these electronic states. Bi-stability has been well studied in the context of magnetic systems, where the spin symmetry provides nearly degenerate ground states. In these systems, the two stable states depend on the internal energy components of the material, such as the magnetic anisotropy, the exchange interactions, and applied external magnetic field. However, little progress has been made in finding bi-stable states involving charge degrees of freedom. Of the three degrees of freedom, charge, spin, and phonons, charge is the fastest and easiest to manipulate. At least, in principle, it should offer a more versatile alternative to spin bi-stability in terms of speed and application.

However, ultrafast bi-stability in electronic systems is difficult to achieve in non-structured materials. Some materials show hysteretic response of the electron conductivity, for example under thermal excitations. However, only one state is strictly stable. The other can be excited by an external stimulus and relaxes back after the stimulus is gone, and is thus not suitable

for ultrafast memory applications. In terms of speed, while transient time to an excited state can occur on the sub-picosecond time scale, there is typically no way to trigger the reverse process (3).

Correlated electron systems offer various pathways of controlling material properties. For example, Vanadium dioxide (VO_2) is an insulator with strong electron-phonon interactions and it undergoes a first order insulator-to-metal transition (IMT) at 340 K (4). At higher temperatures, VO_2 is metallic with the rutile structure (R), while it transforms to the monoclinic M_1 phase and becomes insulating below the transition temperature.

IMT can be achieved on the ultrafast time scale upon laser excitation (5, 6, 7, 8). However, bi-stability is normally not reached as the system undergoes an hysteresis. Whether the transition involves both electrons and phonons, or only electrons, remains a topic of high controversy. The involvement of the lattice is detrimental for ultra-fast switching, as it is typically associated with slow response and high power consumption. In this context, the lattice acts as a dissipation bath (thermal reservoir) that prevents a reversible transition between the metallic and insulating phases (9, 10, 11). Moreover, the nature of the MIT in VO_2 has long been debated, with particular emphasis placed on the role of electron correlations in forming the charge gap. A key unanswered question is whether the IMT is driven by a pure electronic mechanism, as in the Mott transition, or if the Vanadium dimer pairing mechanism driven by Peierls distortions is responsible for the opening of the charge gap (12, 13, 14, 15). This is paramount for future applications, such as low consumption non-volatile memory devices.

Discussion

We use a combination of ultra-fast terahertz (THz) spectroscopy techniques and quasi-particle self-consistent GW theory (QSGW). In the first part, we address the controversy on whether the IMT in VO_2 is purely electronic, or is driven by lattice distortions.

Structural properties are usually probed in equilibrium, and for VO_2 typically at temperatures near T_c . In our experiment, we use 800 nm probe to investigate the ultrafast dynamics immediately following generation of phonons by a THz pump. In this way the dominant excitations well below T_c can be observed. A time resolution below 50 fs is essential to reveal the timescales on which the excited electronic states redistribute their excess energy by coupling with phonons, and in turn can unveil the fingerprint (if any) of specific collective modes associated with the ultrafast rearrangement of the lattice. We performed two different time-resolved measurements: THz-pump, optical probe ellipsometry and THz-pump, optical probe transmission measurements (see Fig. 1). Both can reveal electron densities and phonon oscillations. However, ellipsometry is more sensitive to phonon oscillations (see Fig. 1) and transmission is very sensitive to the electron density. Our sample is a 70 nm-thick VO_2 film on a sapphire substrate.

We first show the spectroscopic ellipsometry measurements carried out along the rutile axis at 800 nm (1.55 eV), for temperatures ranging between room temperature and the transition at 67°C. In Fig. 2.a we show the measured average temperature-transmission hysteresis. As expected, a hysteresis in the transmission is observed, which correlates with the first order transition of VO_2 at 67°C. However, the temporal response is highly non trivial. In Fig. 2.b the birefringence on the optical probe is shown. For all temperatures below 57°C, a coherent temporal response is observed, with three dominant modes at 4.8 THz, 5.7 THz and 6.8 THz (see Fig. 2.b). These frequencies closely match known phonon modes in the M_1 phase near 5 THz (see Table 1 in SI).

Interestingly, the amplitude of these modes also exhibit hysteresis (see Fig. 2.b): the modes survive upon heating to 57°C, but only reappear upon cooling from high temperature at 50°C. The hysteresis of the excitations, however, correlates with the hysteresis obtained in the averaged transmission, which shows that the excitations are an inherent property of the M_1 phase of

VO₂. This also rules out heating effects induced by the THz pulse. The fact that the excitations are present all the way up to the phase transition establishes that the collective excitations are connected to the first order transition of VO₂ and the collapse of the VO₂ gap at T_c . These excitations clearly suggest that the lattice dynamics play a key role for the MI transition, and that the mechanism is Peierls-like, in the sense that changes in electronic states are driven by small nuclear displacements.

Pump-probe Fluence. A fluence analysis (see Fig. 2 in SI) shows the modes' amplitudes vary linearly with the square of the electric field. This establishes that modes are not coherently excited by the THz pump, but involve secondary relaxation mechanisms associated with the coupling of electrons to active phonon modes. With THz spectroscopy, electronic relaxation does not need to obey optical selection rules, but can occur through phonon coupling. We note that the dominant mode is at 5.7 THz.

Optics. To benchmark the QSGW approximation with the experiments, we compute the optical conductivity including ladder diagrams via a Bethe-Salpeter formalism (16). We report in the Fig. 1.b of SI the theoretical optical conductivity along the rutile axis, and the comparison with ellipsometry measurement (17) of σ_x on a single crystal of VO₂. Agreement is excellent up to 4 eV, especially when considering the complexity of this material, and also the variability between different measurements of σ . The optical conductivity is a stringent test of the quality of QSGW, as it is a true *ab initio* theory, free of adjustable parameters.

Phonons. We computed the phonon dynamical matrix at the DFT level (see Table 1 in SI). The theoretical phonon spectrum exhibits three modes in the range 4.8 THz to 7 THz, all of A_g symmetry (denoted here as A_g-I, A_g-II and A_g-III). The phonon frequencies are in excellent agreement with the modes observed by THz spectroscopy, and the phonon eigenvectors supply the nuclear displacements for each normal mode. The A_g-II (A_g-I) involves only displacements of the vanadium (oxygen) atoms, whereas the A_g-III mode involves displacement of both V and

O ions.

Phase diagram. In Fig. 2.d, we report the average transmission at different temperatures. The colour map of the E-field dependent electronic response indicates that, at $T = 57^\circ\text{C}$ near $T_c = 67^\circ\text{C}$, a rapid metallization is suddenly obtained at large electric field $E > E_{\text{threshold}}$ (yellow region). This is also confirmed by the rapid increase of the transmission at large electric fields $E^2 > 0.7$ for $T = 57^\circ\text{C}$ (Fig. 2.e). This has been associated (11) to a threshold field when the absorbed energy density is sufficient to metallize the system via a structural change. In this regime, the monoclinic metallic phase is a dynamic precursor to the rutile metallic state. Fig. 2.d provides a phase boundary in terms of temperatures and electric fields, above which structural changes drive a metallic state. We focus in our work on lower temperatures and electric field, far from the Zener-Keldysh-like interband tunneling (ZKIT) regime.

Electron-phonon interaction. We performed QSGW calculations in a frozen phonon approximation, displacing atomic positions along eigenvectors of each of the three A_g modes 4.81, 5.47, and 6.29 THz. In two of these modes (4.8 and 6.29 THz), a 2-fold rotation around the y axis is preserved, but it is broken for the A_g -II mode (5.47 THz, see Table 1 in SI). Fig. 3.a shows how the quasiparticle band structure evolves for small displacements of either sign ($\delta d \approx \pm 0.022 \text{ \AA}$) in the A_g -II mode. The nearly degenerate pair of d bands just below E_F split in a symmetric manner, independent of the sign of displacement — a characteristic signature of Peierls splitting — while the other bands are largely unperturbed. As a result the gap decreases in proportion to $|\delta d|$ until it closes at $\delta d \sim 0.14 \text{ \AA}$ (Fig. 3.b). Note that a negative Δ_c means that the solution is metallic: the conduction band at Γ overlaps with the valence band, with emergence of electron and hole pockets.

For comparison, a typical high power THz pump will displace ions by roughly 0.1 \AA , while nearest neighbor V-V bond lengths in the rutile and M_1 phase differ by $\sim 0.4 \text{ \AA}$. In the THz experiment, the ions are displaced in a complex manner, so a realistic simulation of the time-

dependence of $\sigma(\omega=1.5\text{eV})$ is not feasible. However, the conductivity $\sigma(\omega)$ is closely connected to independent particle transitions (in particular the structure around 1.5 eV is tied to transitions between the top two valence band states and the unoccupied states), so the initial shape of $\sigma(\omega)$ in the M_1 phase (see Fig. 1b in SI) will evolve with excursions in the band structure (Fig. 1aS) from phonons generated by the pulse. This explains qualitatively the primary features of the THz experiment.

We next turn to the discussion of the A_g -III mode at 6.29 THz. This mode involves an approximately equal displacements of the V and O ions, while preserving the two-fold rotational symmetry around y . The valence band does not split and the charge gap evolves as a smooth function of phonon amplitude u , approaching a small positive value at a critical value we denote as u_c (Fig. 3.c). To provide some measure of the length scales involved, at u_c the nuclei are displaced by an average value of 0.06 Å, though the nearest neighbor V-V bond length increases by only 0.017 Å. As u increases slightly beyond u_c the gap vanishes; the insulating solution becomes unstable at $u_c > u_c$ and the system makes a discontinuous transition to a metallic state, with a indirect negative gap of the order of -0.15 eV, meaning that the conduction band minimum (at Γ) falls slightly below the valence band maximum (which occurs at a low-symmetry point roughly in the vicinity of C). Fig. 3.c displays the evolution of the bands along the Γ -C line.

Bi-stability. Remarkably, at u_c two distinct self-consistent potentials can simultaneously be found *for the same lattice configuration*: one insulating and the other metallic. Both band structures are depicted in Fig. 3.c. This indicates that a purely electronic transition is possible in this system. The M-I transition here is very atypical, in that the associated fluctuations are purely charge-like, without involving the spin. Note that the band structures of the coexisting solutions are similar; however there is a discontinuous change both in Δ_c and the valence band width. The narrowing of the bandwidth in the metallic solution indicates that the system is a

correlated metal.

As a consequence of the coexistence of the two solutions, we obtain a hysteresis; with an excursion in the displacement $u_c < u < u_c'$ the system can remain on one branch or the other. The subtle balance between the localized and itinerant character of the electrons in this regime is a realization of a *spectral-weight scale*: if the valence and conduction bands get slightly closer, the system gets metallic, if they move apart, the system becomes insulating. Note that the M-I transition preserves the optical gap, as the charge gap is indirect. This is distinct from the insulator-metal transition in VO_2 at the critical temperature, where there is a collapse of the optical gap concomitant with a collapse of the charge gap. We note that this process occurs on the time scale of a phonon mode oscillation period, which is typically much faster than the relaxation of resonant electronic excited modes. This opens a pathway for ultra-fast switching processes.

Doped compounds. Finally, we extended the measurements to the case of doped $V_{1-x}W_xO_2$ with $x = 0.01$. We observe that the Ag-III mode is still present upon chemically doping the material, with a much reduced T_c , which opens promising avenues to further tuning the compounds towards the bi-stable phase (see text in SI).

1 Conclusion

We showed that a purely electronically driven transition does not occur for VO_2 at the critical temperature. This concretely addresses a long-standing controversy on the role of phonons in the transition where the M_1 phase of VO_2 is a band insulator with a gap that is too large for pure many-body effects to stabilize a MIT without nuclear displacements.

Nevertheless, with suitable displacements relative to the M_1 phase, a purely electronic MI transition was found unveiling a new IMT mechanism: the Peierls instability which involves an orbital selection, and bonds the d_{xy} and d_{xz} orbitals along the rutile axis, filling each orbital

with one electron. Nuclear displacements around the M_1 phase causes the gap to shrink. When the gap becomes sufficiently small, a purely electronic MIT associated with the 6.8 THz phonon mode arises from the charge fluctuations.

This new mechanism enables bi-stability at room temperature in distorted structures which may be achieved by strain or external doping thus opening new possibilities for materials design under realistic experimental conditions.

Acknowledgments

This work was supported by EPSRC (grants EP/R02992X/1, EP/N02396X/1, EP/M011631/1), and the Simons Many-Electron Collaboration. C.W. gratefully acknowledges the support of NVIDIA Corporation with the donation of the Tesla K40 GPUs used for this research. For computational resources, we were supported by the ARCHER UK National Supercomputing Service and the UK Materials and Molecular Modelling Hub for computational resources (EPSRC Grant No. EP/ P020194/1).

References

1. L. Liu, *et al.*, *Nature Photonics* **4**, 182 EP (2010).
2. Z.-Y. Li, Z.-M. Meng, *J. Mater. Chem. C* **2**, 783 (2014).
3. S. de Jong, *et al.*, *Nature Materials* **12**, 882 EP (2013).
4. F. J. Morin, *Phys. Rev. Lett.* **3**, 34 (1959).
5. C. H. Ahn, J. M. Triscone, J. Mannhart, *Nature* **424**, 1015 EP (2003).
6. Z. Yang, C. Ko, S. Ramanathan, *Annual Review of Materials Research* **41**, 337 (2011).
7. M. Schultze, *et al.*, *Nature* **493**, 75 EP (2012).
8. S. de Jong, *et al.*, *Nature Materials* **12**, 882 EP (2013).
9. A. Cavalleri, *et al.*, *Phys. Rev. Lett.* **87**, 237401 (2001).
10. C. Kübler, *et al.*, *Phys. Rev. Lett.* **99**, 116401 (2007).
11. A. X. Gray, *et al.*, *Phys. Rev. B* **98**, 045104 (2018).
12. M. M. Qazilbash, *et al.*, *Phys. Rev. B* **77**, 115121 (2008).
13. J. H. Park, *et al.*, *Nature* **500**, 431 EP (2013).
14. N. B. Aetukuri, *et al.*, *Nature Physics* **9**, 661 EP (2013).
15. S. Cuffe, *et al.*, *Nature Communications* **6**, 8636 EP (2015).
16. B. Cunningham, M. Grüning, P. Azarhoosh, D. Pashov, M. van Schilfgaarde, *Phys. Rev. Mater.* **2**, 034603 (2018).
17. K. Okazaki, S. Sugai, Y. Muraoka, Z. Hiroi, *Phys. Rev. B* **73**, 165116 (2006).

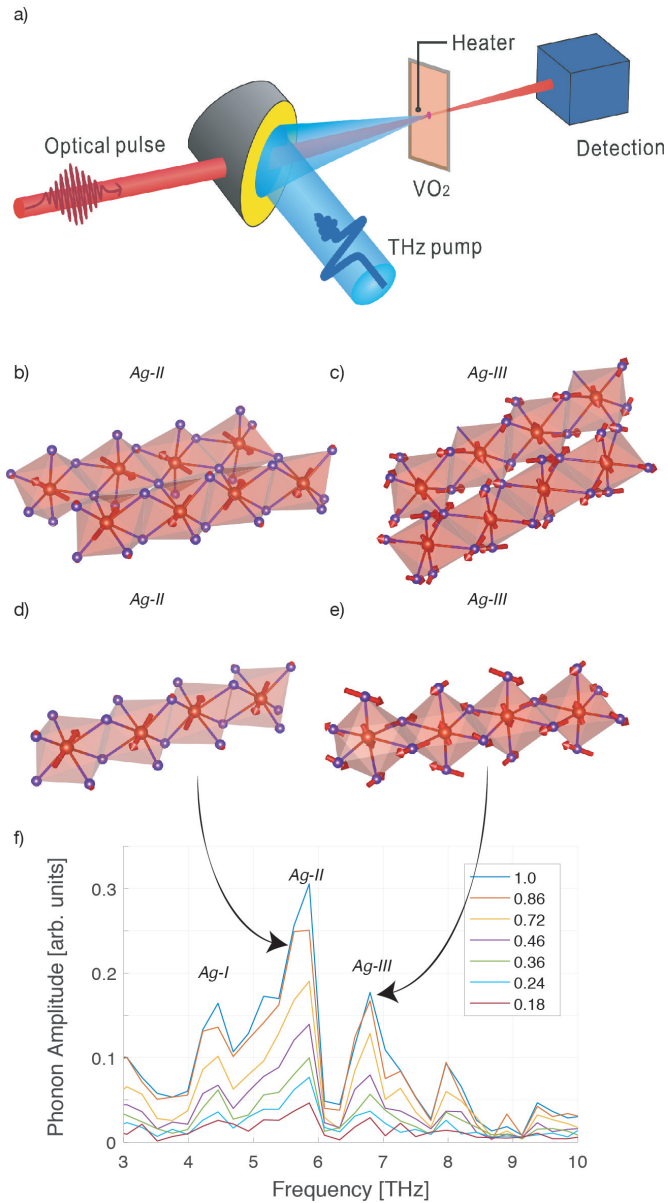


Figure 1: **THz induced lattice distortions far from T_c in VO_2 :** a) The THz pump and optical probe setup. Lattice distortions obtained in the calculated phonon eigenvector modes for b) the 5.7 THz $A_g\text{-II}$ mode and c) the 6.8 THz $A_g\text{-III}$ mode. Panel d) and e) show the enlargement of panel b) and c), respectively, of the V (red spheres) and O (blue spheres) edge-sharing octahedras along the rutile direction. The V-V dimers are located in the center of the rutile chain (second and third positions from the left). f) The amplitude of phonon excitations for different terahertz power levels. The power is normalized by the largest intensity considered in the experiment.

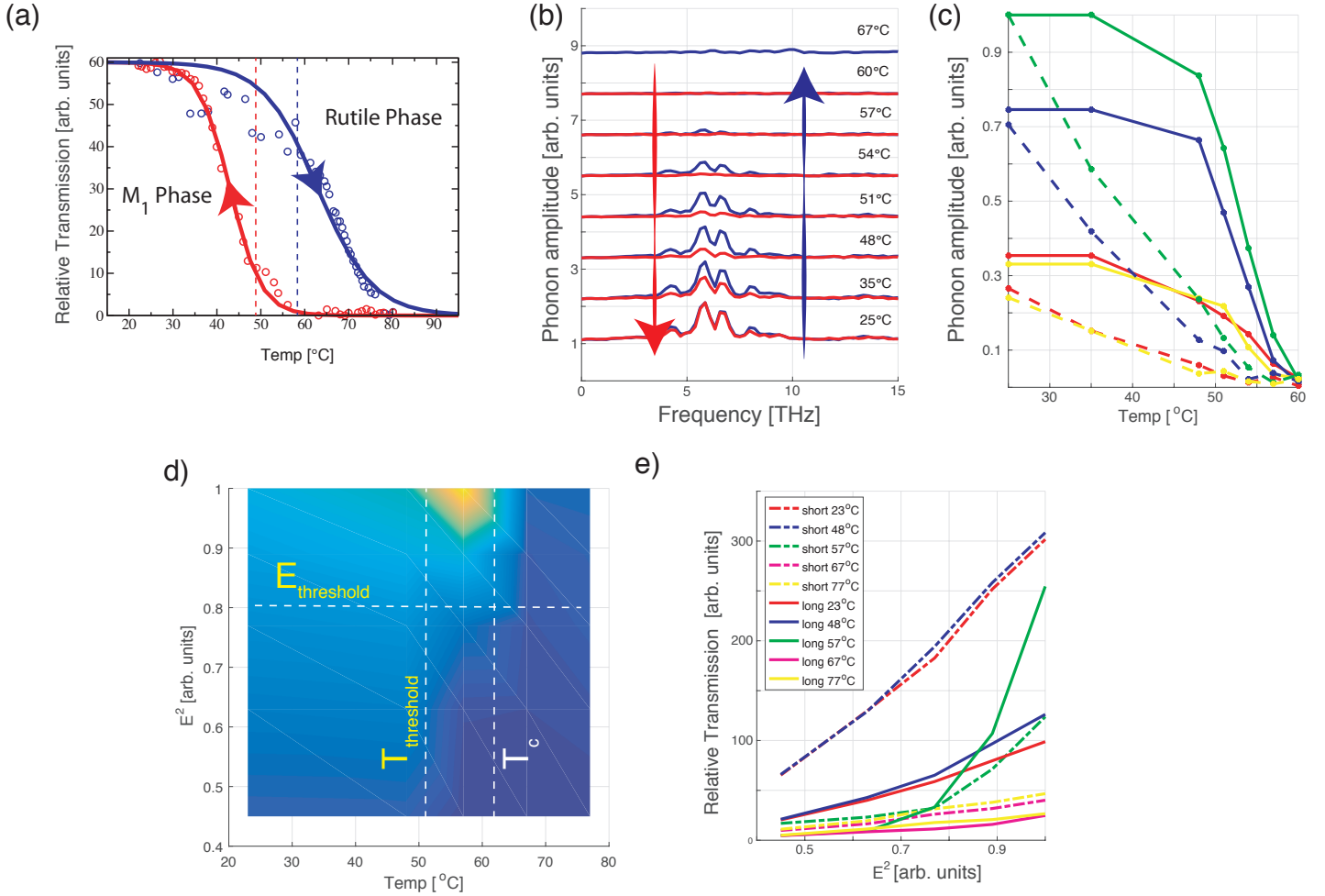


Figure 2: **Ultrafast THz spectroscopy of electron and phonon excitations:** a) Average transmission of the 800nm probe obtained during the heating (blue) and cooling experiments (red). b) Phonon amplitudes obtained by Fourier transform of the time-resolved THz pump optical ellipsometry measurements, at different temperatures between 20°C up to 67°C, normalised by the 5.7 THz mode obtained at 25°C. c) Hysteresis of the phonon amplitudes obtained in b). (d) Phase diagram of the E-field dependent electronic response obtained by time resolved THz pump and optical probe transmission at different temperatures (dark blue for low response, and yellow for high response). At temperature near T_c, $T > T_{threshold}$, and at high electric field $E > E_{threshold}$, the spectra is dominated by a sudden metallization of VO₂ via direct Zener-Keldysh-like interband tunneling (ZKIT). e) Power dependence of the 800 nm transmission at two delay points, respectively instantaneous (short) and at 20 ps (long).

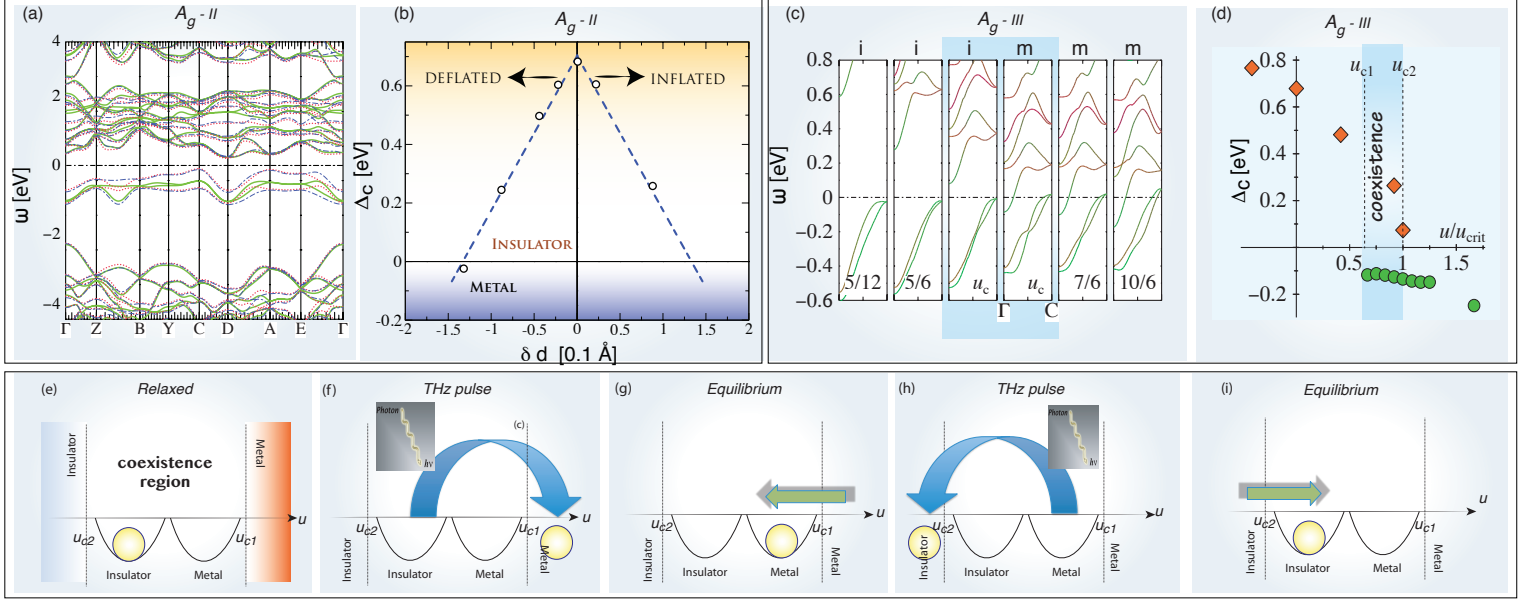


Figure 3: Electronic bi-stability : *a)* QSGW energy band calculations for the displaced structure along the A_g -II (5.47 THz) phonon mode, with both expansions and contractions of the V-V bond ($\delta d \approx \pm 0.022 \text{ \AA}$) (red and blue) around the M_1 phase (green). *b)* The charge gap Δ_c shrinks for either sign of δd and eventually closes for changes in the V-V distance as small as $\delta d \approx 0.15 \text{ \AA}$. *c)* QSGW energy band structure for the A_g -III (e.g., 6.29 THz) phonon mode for displacements above and below the critical displacement u_c , see text. At u_c , QSGW predicts the coexistence of two converged solutions: a metallic solution labelled **m** and an insulating solution labelled **i**. *d)* Charge gap as a function of displacement u : we obtain an hysteresis and purely electronic IMT at u_{c2} (diamonds) and respectively MIT at u_{c1} (circles). Bi-stability is obtained for $u_{c1} < u < u_{c2}$: if we surmise that the nuclear positions of the system can be pinned along the A_g -III mode in the coexistence region, so that the material does not relax to its pristine form, (e) bi-stability would be achieved, and (f) an applied 6.29 THz pulse would drive the system to a metal. After the system relaxed back to the middle region, (g) it would stay in the metallic solution, until (h) another pulse hits the system, after which (i) the system would relax to the insulating solution.